sustainability

MDPI

Article

Experimental and Numerical Research of the Thermal Properties of a PCM Window Panel

Martin Koláček *, Hana Charvátová and Stanislav Sehnálek

The Department of Automation and Control Engineering, Faculty of Applied Informatics, Thomas Bata University, 76001 Zlín, Czech Republic; charvatova@fai.utb.cz (H.C.); sehnalek@fai.utb.cz (S.S.)

* Correspondence: kolacek@fai.utb.cz; Tel.: +420-57-603-5642

Received: 26 May 2017; Accepted: 6 July 2017; Published: 12 July 2017

Abstract: This paper reports the experimental and simulation analysis of a window system incorporating Phase Change Materials (PCMs). In this study, the latent heat storage material is exploited to increase the thermal mass of the building component. A PCM-filled window can increase the possibilities of storage energy from solar radiation and reduce the heating cooling demand. The presented measurements were performed on a specific window panel that integrates a PCM. The PCM window panel consists of four panes of safety glass with three gaps, of which the first one contains a prismatic glass, the second a krypton gas, and the last one a PCM. New PCM window panel technology uses the placement of the PCM in the whole space of the window cavity. This technology improves the thermal performance and storage mass of the window panel. The results show the incongruent melting of salt hydrates and the high thermal inertia of the PCM window panel. The simulation data showed that the PCM window panel and the double glazing panel markedly reduced the peak temperature on the interior surface, reduced the air temperature inside the room, and also considerably improved the thermal mass of the building. This means that the heat energy entering the building through the panel is reduced by 66% in the summer cycle.

Keywords: phase change material (PCM); thermal cycle test; supercooling; calorimetric chamber; incongruent melting; thermal imager

1. Introduction

In recent years, phase change materials (PCMs) have become more popular in different building components such as underfloor heating [1], cooling ceilings [2], PCM wallboards [3,4], and especially in glazing systems [5–8]. This is thanks to their increasing the thermal inertia of the construction. These materials have a melting point in the area of the comfort in the building and they stabilize temperature fluctuations and reduce overheating on summer days.

According to their chemical composition, PCMs are divided into three main groups: organic compounds, inorganic compounds, and inorganic eutectics. Each group of PCMs has its typical properties, different melting points, and different applications as described in [9]. It is important to match the suitable temperature range for the PCMs for a given application. PCM energy storage systems are based on these aspects [10]. Some recent studies have concerned PCMs with a different chemical composition in glass systems [2,5–7]. As evident from these studies, different PCM compounds cause the different behavior of the PCM inside the glass system.

The architectural design of buildings increasingly uses glass structures. These building elements increase the heat load and increase cooling requirements. Reducing the heat transfer of solar radiation is possible with reflective elements such as a prismatic glass. PCMs allow the reduction of temperature fluctuations and the storage of excess energy that are primarily caused by solar gains. The combination of reflective elements and PCMs is able to achieve thermal comfort and reduce cooling requirements

inside buildings. The subject of our research is the use of a specific glass elements using prismatic glass and a PCM. Solar radiation is reflected by the prismatic glass >40° but allows winter solar radiation to pass <35°. The solar transmittance of the PCM window is 11% for solid state and 15% for liquid state as described in [6]. These results show no relevant difference in the direct solar transmittance between the solid and liquid states. The minimal effect of the solar transmittance can be explained the complex structure of the glazing, where the PCM layer has a much lower impact on the total behavior of the window panel [6].

New PCM technology exploits its application into the entire cavity of the glass. Previous PCM technology used a polycarbonate segment that contained the PCM, as described in [6]. This new technology improves the thermal performance and storage mass of the window panel. However, hydrate salts are present in a large volume and they can lead to incongruent melting. Salt hydrates consist of several components, at least one salt and water, that separate into different phases and thus show problems with cycling stability as described in [11]. Salt hydrates have significantly higher vapor pressures. These pressures could induce water loss and progressive change of their thermal behavior [12]. Therefore, the cavity of the window contains open space for the volume change from solid to a liquid that can be up to 10% of volume.

Calcium chloride hexahydrate $CaCl_2 \cdot 6H_2O$ was selected as the PCM in this experimental research. The use of this hydrate salts as a PCM was first proposed in 1951 by John R. Swanton. As described in [13], the PCM was tested for long-term stability. No change in thermal properties was found after 5650 cycles of melting and solidification. The thermal cycles of calcium chloride hexahydrate are described in [13]. The repeated thermal cycles showed an interesting stability of thermal properties i.e., the latent heat of fusion and the melting temperature. The thermal cycle tests were conducted by Differential Scanning Calorimeter. A large amount of this material represents changes in the process of melting and solidification.

Nevertheless, this material exhibits incongruent melting and supercooling tendencies [14]. Incongruent melting causes uneven melting and it can consequently cause hydrate solids buildup. This crust impedes the heat release from the PCM and deteriorates the supercooling.

Supercooling is a state when PCMs do not solidify immediately upon cooling below the melting temperature: the crystallization starts when the temperature of the PCM is well below the melting temperature [12,15]. As can be seen in Figure 1, the supercooling effect deteriorates the properties of the material. If nucleation does not happen, the latent heat is not released and the material only stores sensible heat [16]. Some materials achieve supercooling at temperature differences ranging from a few degrees up to 20 °C. The reason for the high degree of supercooling is the rate of nucleation of crystals from the melt or the rate of growth of these nuclei or rate of both process is very slow. High-viscosity materials in the liquid state have low diffusion coefficients for their constituent atoms. These atoms can be unable to rearrange themselves to a solid; instead, the liquid undergoes supercooling [10].

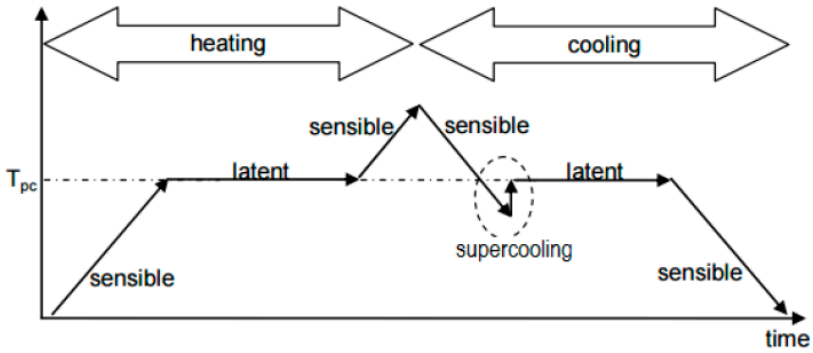

Figure 1. Temperature change during heating and cooling of a Phase Change Material (PCM) with a supercooling effect [11].

The study [17] confirmed the supercooling effect of the calcium chloride hexahydrate between approximately 1 to 3 degrees Celsius.

In this paper, the first section presents methods used for measuring the heat transfer by conduction by the melting process of the PCM inside the window. The second section presents the results of measurement of the PCM window panel in the double calorimetric chamber where the window panel was exposed to different temperatures. Finally, a simulation model of PCM window panel was created in the COMSOL Multiphysics. The model of the PCM window panel was performed to evaluate the impact of the window on the internal microclimatic condition of the room and also to compare it with a double-glazing system.

2. Methods

The measurement of heat transfer energy was performed on the specific glazing system in which a PCM is used to stabilize the climatic conditions in the indoor environment. The aim of this study was to measure the heat transfer by conduction through the window panel during the different microclimatic conditions. The window panel contains a PCM material that markedly decreases the solar transmission. Accordingly, it was important to verify the melting process of the PCM. The total surface thermal transmittance of the glazing defined the heat transfer through the window as described by the standard (EN 673 Determination of thermal transmittance). The thermal transmittance U value is defined according to BS 6993-1: (1989) the heat flux density through a given structure divided by the difference in environmental temperatures on either side of the structure in steady-state conditions. The thermal transmittance of the window is calculated for the inside heat transfer coefficient, the outside heat transfer coefficient, and the total heat transfer coefficient that incorporates radiative heat transfer through the window. The thermal transmission of the window is calculated by thermal transmission caused by the radiation and thermal transmission of the given gas and the PCM thermal transmission. The heat transfer coefficient is used in calculation the heat transfer typically by convection. Nevertheless, the heat transfer coefficient of the PCM is temperature-dependent and it is very difficult to determine heat transfer during the phase change of the PCM.

2.1. Instrumentation

The dimensions of the window panel are 1 × 1 m and 0.085 m in thickness. It consists of a four-pane glazing package as is shown in Figure 2. The prismatic glass solar reflection device is placed in the outermost cavity, the second cavity is filled with krypton gas, and the innermost cavity is filled with the PCM. The main goal of testing was to achieve the characteristic behavior of the PCM in the case that the outside air temperature grows up to the melting point of the PCM. The melting point presents the important thermal property of the PCM (Calcium chloride hexahydrate). Figure 2 shows the sections of the window panel. These sections and their composition cause the high weight of the window panel (i.e., 95 kg). The density of Calcium chloride hexahydrate is 1562 kg/m^3 for liquid state and 1710 kg/m^3 for solid state.

Due to the massive construction of the glass panel, one of the measurements had to be done by attaching the glass panel to the existing glass construction, where the surface temperature on the both sides of the panel was measured. We tested the PCM window panel under different conditions and in a compensated calorimetric chamber to see if the PCM inside the cavity of PCM glass panel can melt in its entire volume.

The measurement device is a Compensated Calorimetric Chamber whose primary use is testing the energy and acoustic parameters of cooling units; air/air and air/water heat pump units, cooling ceilings and cooling beams, selected heating elements, and other building equipment. It consists of four parts, including the indoor and the outdoor sides, which each has compensated thermal control interspace as shown in Figure 3. This compensated space always has the same temperature as the inner space, which ensures minimum heat loss to the outer space. The only heat transfer is through the partition wall between the indoor and outdoor spaces. All spaces have heat exchangers for temperature

control connected to water-glycol distribution, ensuring temperature control between 5 °C to 40 °C. Electric heaters are also provided. The outdoor part has an additional direct chiller and its temperature can be maintained down to −30 °C. Humidity control is also provided and can be controlled in the range from 5% to 95%. All energy sources of cold or heat are designed to provide enough power up to measure units with the power of 20 kW.

The characterization of the partition wall was conducted by the calibration test. The test allowed the definition of heat dispersion through the partition wall between the indoor and outdoor chambers. The measurement of the thermal transmittance of the window is described in references [18,19].

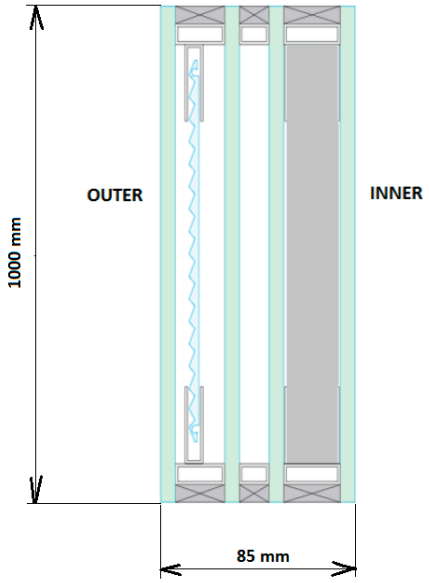

Figure 2. Structure of the tested PCM window panel.

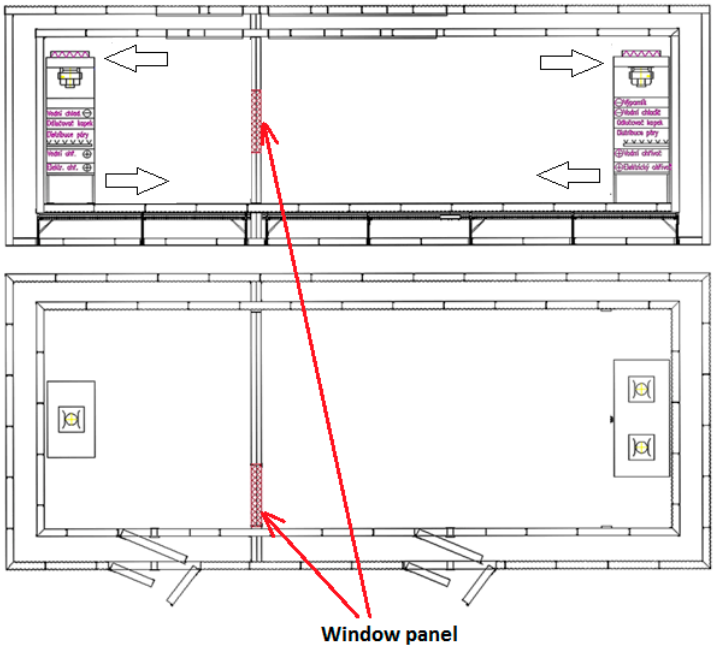

Figure 3. Scheme of the compensated calorimetric chamber where the PCM window panel was installed.

Temperatures and heat flows were continuously monitored during the experiment. The heat flow was measured using Heat flow FQA on each side of the window panel. These heat flow meters have a measurement accuracy of ± 0.05 W/m^2. The heat flow meters are equipped with thermocouple with multiple contacts that make it possible to measure the temperature difference on both sides of the heat flow meter. The surface temperatures were measured by thermocouples in four positions on each side of the window panel. The thermocouple wires were lead along isotherm to reduce the heat conduction effects. A reflective aluminum foil was placed as a radiation shield over the sensors, leaving a ventilated cavity between the foil and the sensor. The surface temperature was also measured by thermal imager (Fluke Ti45), which was used to monitor the internal surface of the PCM window panel.

2.2. Numerical Simulations

The finite element method was used to predict the effect of a heat transfer through the PCM window panel. The model of the PCM window panel was created and tested under various thermal conditions. All the simulations were realized with the Heat Transfer Module in COMSOL Multiphysics.

The initial conditions of the simulation were measured in the real laboratory at Faculty of Applied Informatics TBU in Zlín in the Czech Republic. The computer simulation also tested the model of the laboratory where the glass system with the PCM was applied. The first part of this study consists of the comparison of measured and predicted temperatures in the laboratory in order to assess the PCM window panel's ability to decrease the maximal air temperature inside the building.

The input parameters—the inside air temperature, the outside air temperature, and the solar radiation—were measured in the laboratory. These parameters specify the results in the simulation model and obtained the thermal parameters of the window panel. Table 1 shows the physical properties of the window materials. The amount of absorbed heat energy depends mainly on the thermal capacity of the PCM. The thermal capacity and the thermal conductivity are a function of the temperature of the PCM. The specific thermal capacity is measured by differential scanning calorimeter as described in [20].

Table 1. Physical properties of the windows materials.

Material	Thermal Conductivity [W·m^{-1}·K^{-1}]	Density [kg·m^{-3}]	Spec. Thermal Capacity [J·kg^{-1}·K^{-1}]
Tempered safety glass	0.76	2600	840
Prismatic glass	0.76	2600	840
Krypton	0.00943	3.749	248
Window frame	0.3	1210	1800

The simulation model of the PCM window does not allow to simulate the phase separation process between liquid and solid phases. Specific thermal capacity and thermal conductivity were implemented in the simulation model.

The COMSOL Multiphysics was validated by the model of the steady-state and transient ground-coupled heat test cases specified in the International Energy Agency Building Energy Simulation Test (IAE) by a methodology developed by Ron Judkoff. The combination of empirical validation, analytical verification, and comparative analysis techniques are main procedures of this methodology. It describes six cases of ground-coupled heat transfers test cases designed to be compared with verified whole building energy simulation software. Several of those already tested by IEA are EnergyPlus, FLUENT, Matlab, TRNSys, GHT and ANSYS Fluent. As you can see in [21] COMSOL Multiphysics was validated at authors department, where simulated data showed agreement with the rest energy simulation software as well as with analytical solution.

2.2.1. Finite Element Equations for Heat Transfer in the Window Panel

A basic equation of non-stationary heat transfer in an isotropic body can be described by Equation (1),

$$-\left(\frac{\partial q_x}{\partial x}+\frac{\partial q_y}{\partial y}+\frac{\partial q_z}{\partial z}\right)+\Phi=\rho c_p\frac{\partial\theta}{\partial t} \quad (1)$$

where

q_x, q_y, q_z	components of heat flow density	($W{\cdot}m^{-2}$),
$\varphi = \varphi(x, y, z, t)$	inner heat-generation rate per unit volume	($W{\cdot}m^{-3}$),
ρ	material density	($kg{\cdot}m^{-3}$),
c_p	heat capacity	($J{\cdot}K^{-1}$),
θ	temperature	(K),
t	time	(s).

According to Fourier's law, the components of heat flow can be expressed as follows [22]:

$$q_x=-\lambda\frac{\partial\theta}{\partial x},\quad q_y=-\lambda\frac{\partial\theta}{\partial y},\quad q_z=-\lambda\frac{\partial\theta}{\partial z} \quad (2)$$

where λ thermal conductivity ($W{\cdot}m^{-1}{\cdot}K^{-1}$).

Substitution of Fourier's relations Equation (2) into Equation (1) gives the basic heat transfer Equation [21]:

$$\frac{\partial}{\partial x}\left(\lambda\frac{\partial\theta}{\partial x}\right)+\frac{\partial}{\partial y}\left(\lambda\frac{\partial\theta}{\partial y}\right)+\frac{\partial}{\partial z}\left(\lambda\frac{\partial\theta}{\partial z}\right)+\Phi=\rho c_p\frac{\partial\theta}{\partial t} \quad (3)$$

It is assumed that the boundary conditions can be of the following types [22]:

1. Specified temperature: $\theta_s = \theta_1\ (x, y, z, t)$ on S_1.
2. Heat flow density: $q_s = q(x, y, z, t)$ on S_2.
3. Convection boundary conditions: $q_x n_x + q_y n_y + q_z n_z = h\ (\theta_s - \theta_e) + q_r$ on S_3.
4. Boundary condition describing heat transfer in ideal body contact: $\lambda_1\frac{\partial\theta_1}{\partial n} = \lambda_2\frac{\partial\theta_2}{\partial n}$
5. Radiation $q_x n_x + q_y n_y + q_z n_z = \sigma\varepsilon {T_s}^4 - \alpha q_r$ on S_4.

where

h	heat transfer coefficient	($W{\cdot}m^{-2}{\cdot}K^{-1}$),
θ_s	unknown surface temperature	(K),
θ_e	convective exchange temperature	(K).
q_r	incident radiant heat flow per unit surface area	($W{\cdot}m^{-2}$),
q_x, q_y, q_z	components of heat flow density	($W{\cdot}m^{-2}$),
σ	Stefan-Boltzmann constant	($W{\cdot}m^{-2}{\cdot}K^{-4}$),
ε	surface emission coefficient	(−),
α	surface absorption coefficient	(−).

For initial temperature field for a body at the time $t = 0$ it holds [21]:

$$\theta(x, y, z, t) = \theta_0(x, y, z) \quad (4)$$

2.2.2. Numerical Modeling of Phase Change Materials

During the phase change process of the PCM encapsulated in a porous building material can exist in three states: Solid, Liquid, and "Mushy" (the coexistence of both phases). The heat transfer process of the PCM is complicated in construction, especially when the PCMs are in a transition state. The thermal properties of a matrix of construction material are different from the constituent properties. The numerical model of the PCM window panel is simplified due to the fact that the COMSOL Multiphysics is not able to solve heat transfer during the complex crystallization and melting

of the salt hydrate. However, the simulation model of the PCM window panel simply illustrates the heat transfer in a complex window element in order to compare it with a simple window element.

Differential equations of transient heat conduction with variable thermos-physical properties can be described by Equation (5) as described in [23],

$$\frac{\partial}{\partial t}\cdot\rho(\theta)\cdot h(\theta) = \nabla\left[\lambda(\theta)\cdot\nabla\theta\left(\vec{x},t\right)\right] + g\left(\vec{x},t\right) \quad (5)$$

where

h	specific enthalpy	($J\cdot kg^{-1}$),
g	heat generation rate	(W),
x	spatial coordinates	(m).

2.2.3. Enthalpy Method

Modelling of phase transient is used by methods of enthalpy and the method of effective heat capacity.

The latent heat is included to the function enthalpy. The enthalpy expresses heat that contains a unit amount of substance. It can be generally explained by Equation (6) as is described [24],

$$H = \int_{\theta_i}^{\theta} \rho\cdot c\cdot d\theta + L \quad (6)$$

where

H	volumetric enthalpy	($J\cdot m^{-3}$),
c	thermal heat capacity	($J\cdot kg^{-1}\cdot K^{-1}$),
L	latent heat	($J\cdot m^{-3}$).

2.2.4. Effective Heat Capacity Method

The heat capacity includes latent heat of phase change. Therefore, the function of heat capacity sharply increases or decreases in the peak of phase change of the material. An advantage of this method is the primarily dependence on temperature. This method eliminates fluctuations of method enthalpy [25]. It is important to determine the effective heat capacity of this method according to the results of differential scanning calorimetry [4]. The effective heat capacity is calculated by the Equation (7),

$$C_{eff}(\theta) = \frac{dh}{d\theta} \quad (7)$$

where

C_{eff}	effective heat capacity	($J\cdot kg^{-1}\cdot K^{-1}$),
h	enthalpy	($J\cdot kg^{-1}$).

Heat transfer in the integration of effective heat capacity can be described by the Equation (8),

$$\rho(\theta)\cdot c_{eff}\frac{\partial\theta}{\partial t} = \nabla\left[\lambda(\theta)\cdot\nabla\theta\left(\vec{x},t\right)\right] \quad (8)$$

where

x	spatial coordinates	(m).

As the relationship between specific heat capacity and temperature in isothermal problems involves sudden changes, the zero-width phase change interval must be approximated by a narrow range of phase change temperatures. When the material properties are not dependent on temperature,

parameters should be obtained during the consideration that the phase change occurs in a narrow temperature interval [25]. In this case, the heat capacity can be expressed by Equation (9),

$$c_{eff} = \begin{cases} c_{ps} \ldots\ldots\ldots\ldots\ldots\ldots\ldots\ldots\ldots\ldots \theta < \theta_m - \Delta\theta_m \\ \frac{c_{ps}+c_{pl}}{2} + \frac{l_{pl}}{2 \cdot \Delta\theta} \ldots\ldots\ldots\ldots\ldots\ldots \theta_m - \Delta\theta_m \leq \theta \leq \theta_m + \Delta\theta_m \\ c_{pl} \ldots\ldots\ldots\ldots\ldots\ldots\ldots\ldots\ldots\ldots \theta > \theta_m + \Delta\theta_m \end{cases} \quad (9)$$

where

c_{eff}	effective heat capacity	($J \cdot kg^{-1} \cdot K^{-1}$),
c_{ps}	average heat capacity-solid	($J \cdot kg^{-1} \cdot K^{-1}$),
c_{pl}	average heat capacity-liquid	($J \cdot kg^{-1} \cdot K^{-1}$),
l_{pl}	the heat of phase change per unit weight	($J \cdot kg^{-1}$),
θ_m	the phase change temperature solid-liquid	(K),
θ	the temperature of storage medium	(K),
$\Delta\theta_m$	the temperature semi-interval across θ_m	(K).

2.2.5. Effect of the PCM Window Panel on Indoor Air Temperature and Comparison with a Double-Glazing Window

The double-glazing window was tested and was consequently compared to the model of the PCM window panel. The output data from the simulation model were only limited by the fact that the air temperature of the surrounding rooms of the laboratory was stable. The simulation data show the effect of the heat accumulation of the window panel in the room. The results of the PCM window panel are shown in Figure 10, where they are compared with the commercial glazing system.

3. Results

3.1. Experimental Measurement on the Glass Construction

Figure 4 shows temperatures of the PCM window panel and room temperatures inside and outside the room on a sunny summer day. As can be seen in Figure 4, the maximum temperature of the outside surface of the window panel rose dramatically up to 65 °C. The outdoor air temperature constantly fluctuated in the range from 10 °C to 23 °C. Nevertheless, the solar radiation caused the large-scale temperature fluctuation on the outside surface of the window panel. The temperature difference between the outer and inner surface of the window panel was caused by its composition. The third cavity of the window panel is filled with a PCM; this material has low thermal conductivity, which improves the insulation property of the window. The application of the PCM material considerably decreased the heat transfer through the window panel. Although the indoor temperature grew slightly, as is shown in Figure 4, it was due to thermal properties of the tested room. The tested room was furnished on all four sides by traditional triple glazed windows. Consequently, the indoor air temperature was steadily affected. Nevertheless, the results confirm both the high efficiency of the heat storage energy of the PCM window and the improvement of insulation properties of the entire building. The high surface temperature on the interior was caused the high air temperature inside the room.

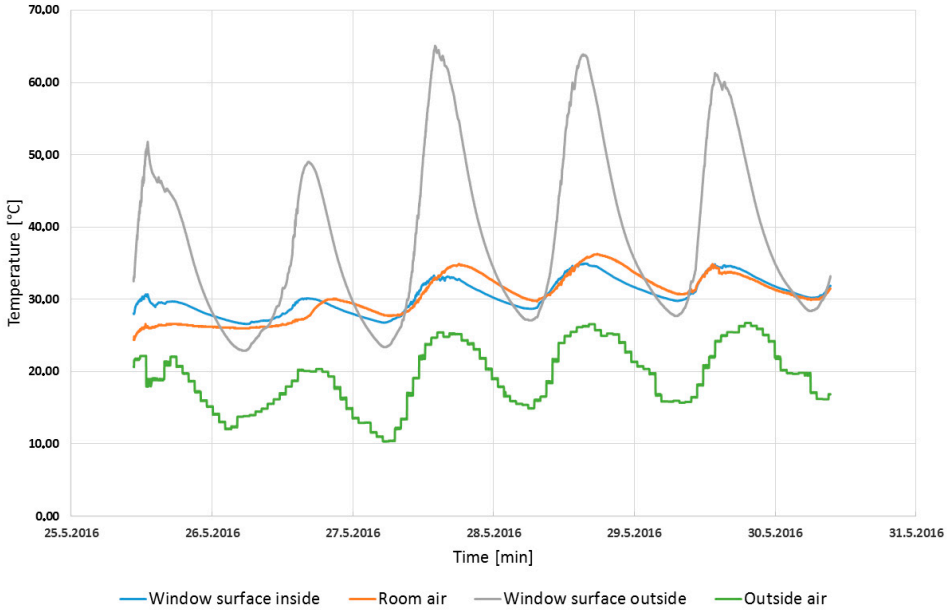

Figure 4. Surface temperature of the PCM window and surrounding air temperature.

3.2. The Melting Process

The results of the melting process of the calcium chloride hexahydrate in the PCM window panel is shown in Figure 5. Salt hydrate consists of an anhydrous salt with corresponding crystal water. These elements consequently caused a typical phase separation as can be seen in Figure 5. Figure 5 shows a sediment of the melting process (left) and the second result (right). As can be seen in the photos, the sediment grew with the repeated cycle of melting (third cycle). The PCM glass panel contained the PCM material in the whole space of the cavity and caused incongruent melting. An incongruently melting salt hydrate consisted of an anhydrous salt with corresponding crystal water [14]. The PCM involves a seed crystal that triggers the solidification of the PCM. This problem is described in [11]. This effect of recrystallization also decreases the risk of supercooling.

In the second measurement, the PCM window panel was located in the calorimetric chamber and the air temperature was 22 °C. However, the result confirmed the supercooling effect that caused a total solidification of the PCM within three days. During the discharge period of the PCM, the heat did not effectively release from the PCM into the room.

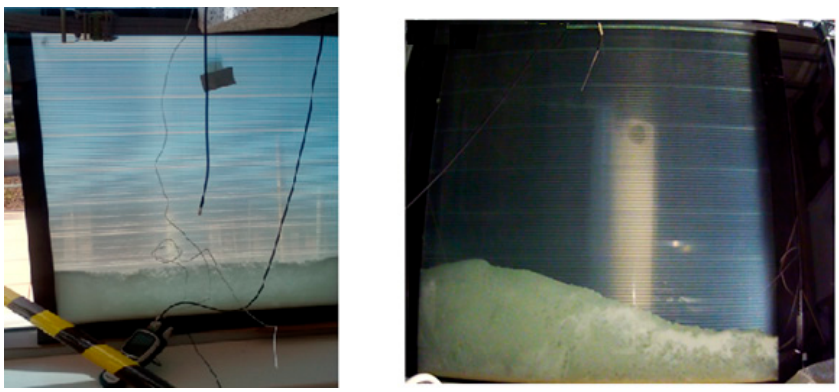

Figure 5. The melting process of the PCM glass panel, the picture on the **left** shows first melting process. The picture on the **right** shows second melting process of the PCM window panel in the calorimetric chamber.

3.3. Measurement in the Calorimetric Chamber

As can be seen in Figure 3, the PCM window panel was located in the partition wall of the calorimetric chamber. The thermal parameters of the partition wall were obtained in the calibration experimental procedure of the calorimetric chamber. This procedure determined the heat flow through the partition wall in different climatic conditions. Thermal transmittance of the window is measured as describe [16,19].

The heat loss and the thermal transmittance of the partition wall were established according to the calibration procedure. During the testing of the PCM window, the temperature difference was 15 °C between the Indoor and the Outdoor section of the chamber and the performance of heat loss was 160 W. The thermal transmittance of the partition wall is 0.13 $W/m^{-2}{\cdot}K^{-1}$ as is shown in Table 2.

Table 2. Determined properties of the partition wall.

Variable	Value	Unit
Thermal resistance	7.42	$[m^2{\cdot}K{\cdot}W^{-1}]$
Thermal conductivity	0.027	$[W{\cdot}m^{-1}{\cdot}K^{-1}]$

3.4. Solidification Process

Figure 6 shows the PCM crystallization process under specific thermal conditions in the chamber. The outdoor air temperature was stable at −15 °C, and the blue curve in Figure 6 represents the indoor air temperature 20.5 °C. The red curve is the average surface temperature of the glass, and the yellow curve is the average surface temperature of the glass in the area of the sediment. The start of crystallization shows on the red curve when the temperature sharply grew in time 14:20. The temperature of sediment (yellow curve) is higher than the surface temperature on the glass (red curve) because the sediment was in a solid state and could not absorb energy as the part in a liquid state. The surface temperature of the sediment decreased more rapidly than the surrounding surface temperature and achieved the temperature difference of 2 °C. The sediment acted as a thermal insulator at the beginning of the crystallization process, as can be seen in Figure 6. The temperature difference between the curves of the glass and the glass-sediment indicates the deterioration of the heat release from the PCM and the missing nucleation agents that caused incongruent melting and the formation of the sediment. The temperature difference is evident from the thermogram in Figure 7, which shows the surface temperature of the entire surface of the PCM window panel. The thermogram showed an almost 5 °C temperature difference. Both measurements confirmed the lower temperature on the sediment, which was caused by incongruent melting. The sediment of the salt hydrate covered the space of the window panel by 25%, as shown in Figure 8. The producer states that the light transmission of the window for liquid state of the PCM is max. 45%, for the crystalline PCM 28%. Due to the prismatic glass, the window panel mainly transmits diffuse irradiation. Therefore, the sediment causes a reduction of diffusion irradiation. Nevertheless, the incongruent melting can still increase the sediment and aggravate the heat accumulation properties of the window and the diffusion irradiation.

The results also show the supercooling effect, wherein the crystallization process begins when the surface temperature of the glass achieved 21.2 °C. It is impossible to measure the temperature of the PCM inside the window. Nevertheless, the supercooling effect is evident.

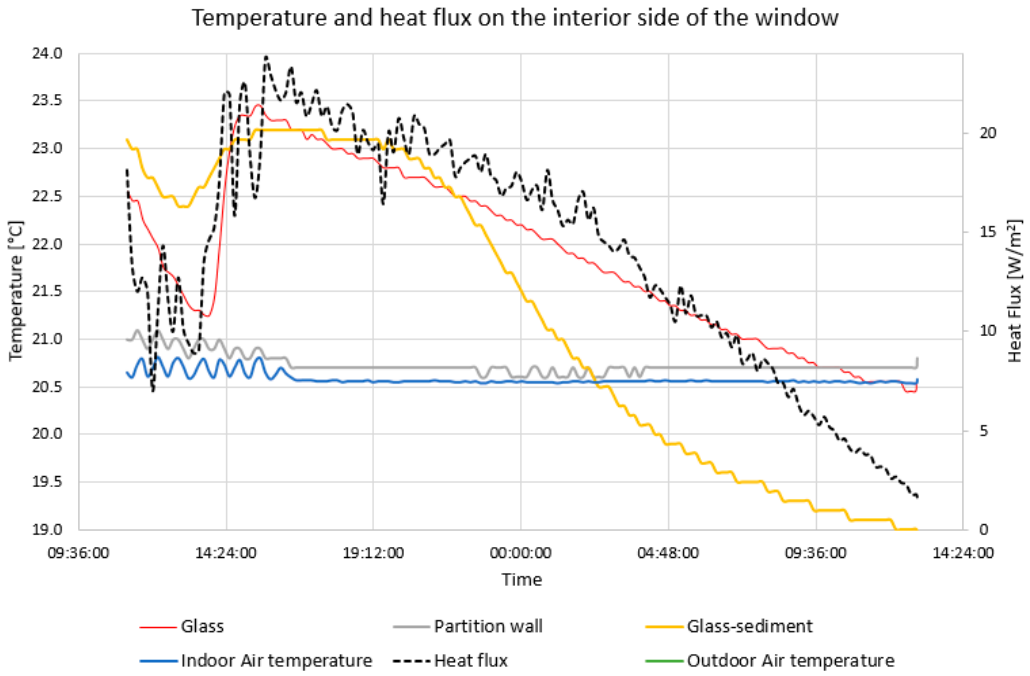

Figure 6. Surface temperature and heat flux on the interior side of the window panel during the climatic test. The indoor air temperature was 20.5 °C and the outdoor air temperature was −15 °C.

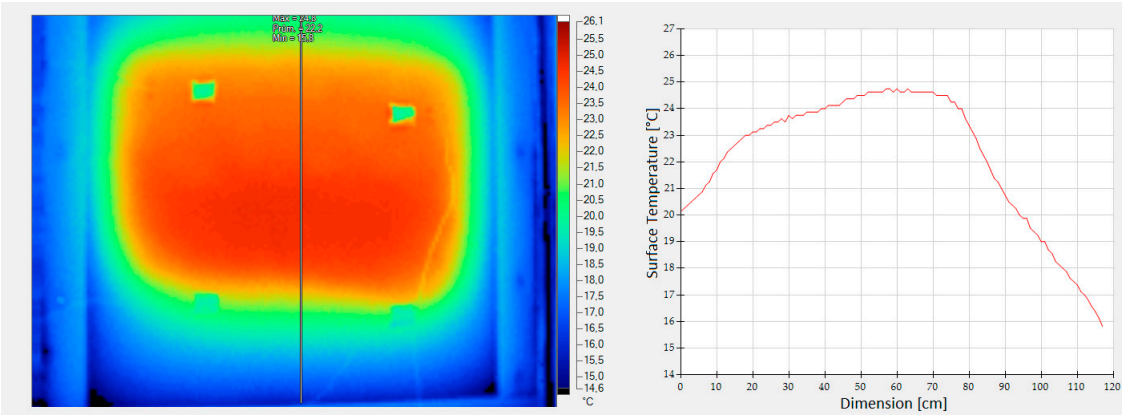

Figure 7. Thermogram of the PCM window panel during the solidification.

Figure 8. The sediment inside the PCM window panel.

3.5. Simulation Model of the PCM Window Panel

The simulation data showed the high thermal insulation of the individual parts of the PCM window panel and especially high storage capacity. The simulation was performed to evaluate the internal temperature and temperature stratification of the PCM window panel. However, this is a simplified model situation that does not involve a phase change of the storage substance but only shows the differences in thermal inertia of the PCM window panel and double glazing panel. The outside air temperature, the inside air temperature, and the solar radiation were measured for four days in July 2016 to use as conditions for simulation, as shown in Figure 9. The results of solar radiation were recalculated from the horizontal solarimeter by the CSN 730548 Calculation of thermal load of air-conditioned spaces [26]. The heat transfer coefficient on the inside 8 $W \cdot m^{-2} \cdot K^{-1}$, on the outside 14 $W \cdot m^{-2} \cdot K^{-1}$ and the emissivity of both sides was set to 0.89. All these parameters were used as boundary conditions in the simulation model.

The simulation results of the PCM window panel was almost the same as the results of the measurement as describes Section 3.1. Due to the high air temperature inside the room the surface temperature on the interior side was higher on the real window panel than in the simulation model.

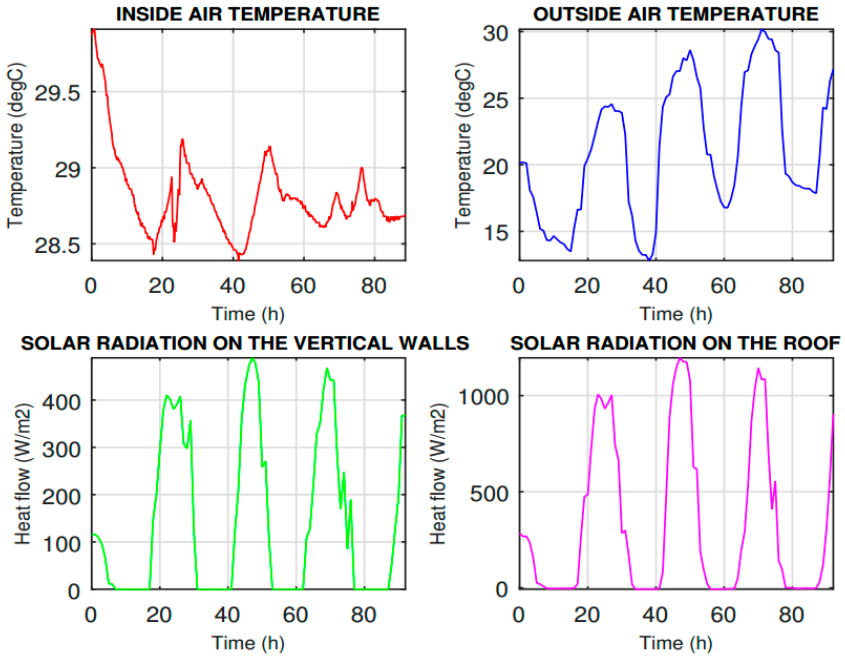

Figure 9. The boundary conditions of the simulation model—measured and calculated values of the inside and outside air temperatures, solar radiation.

Figure 10 shows comparison of the thermal distribution of the temperature distribution in the PCM window panel and double glazing panel, where the initials conditions of the PCM window panel were 25 °C on the inside and 29 °C on the exterior of the PCM window panel.

As can be seen in Figures 10 and 11a during four days the heat energy did not transfer through the PCM window instead of the double glazing panel Figure 10b, the surface temperature on the inside reached up to 37 °C.

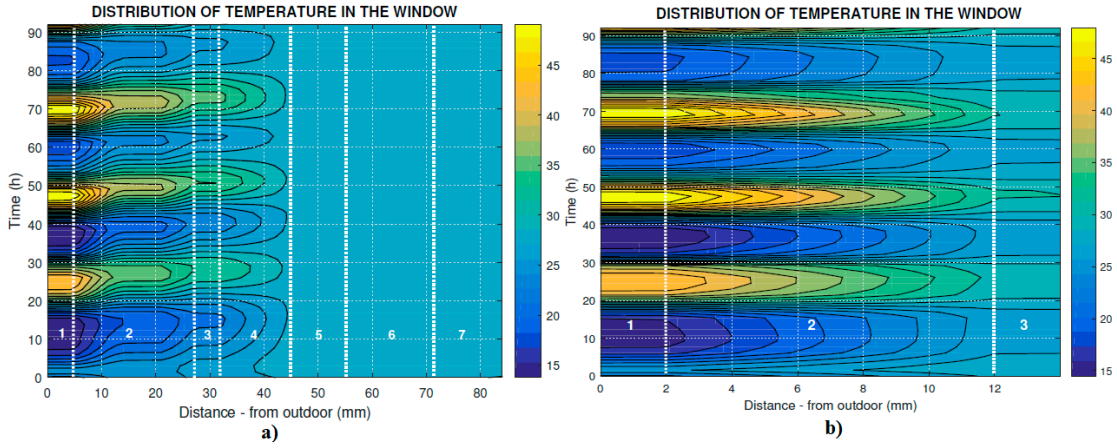

Figure 10. Distribution of temperature in (**a**) PCM window panel; (**b**) Double-glazing panel, from the exterior to the interior.

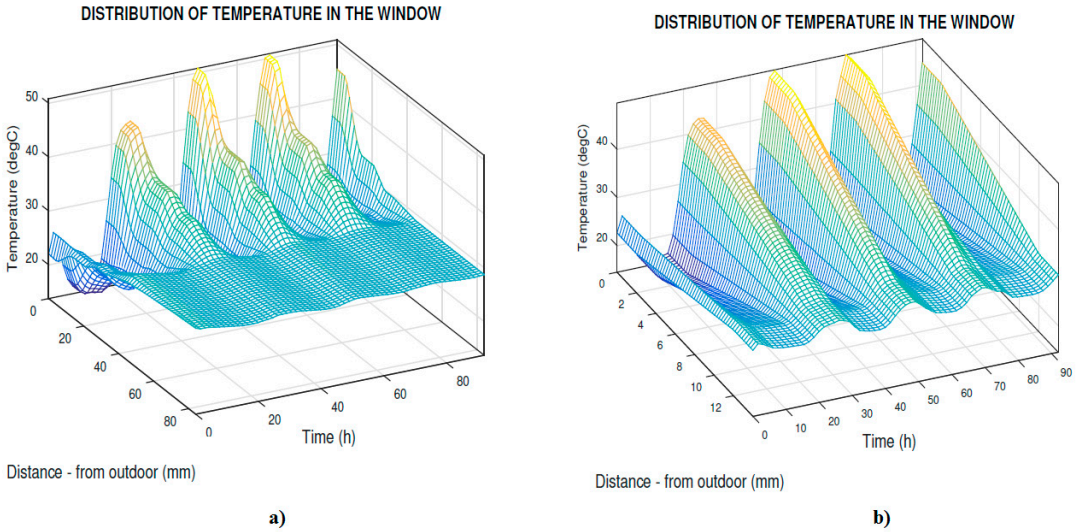

Figure 11. 3D Temperature stratification in the window (**a**) PCM window panel; (**b**) Double-glazing panel, from the exterior to the interior.

4. Discussion

Testing of the PCM window panel affirmed the incongruent melting of salt hydrates that filled the whole cavity of the window panel. The use of the calorimetric chamber shows the high thermal inertia of the PCM window panel during different thermal conditions. Previous technology [6] causes the non-linear behavior of the PCM layer because of usage of a polycarbonate encapsulated PCM. Due to this, we measured the surface temperature in several places with thermocouples and a thermal imager. Nevertheless, the results confirmed that the PCM window panel without polycarbonate containers caused the rise of the sediment in the cavity of the window panel. The thermal test of melting was performed for 10 times where the window was exposed to high temperature for 20 h during each cycle. The sediment was created during each melting cycle. The measurement confirmed problematic placement of the PCM inside the window.

It should be noted that this study was only concerned with the thermal behavior and the thermal inertia of the PCM window system under different climatic conditions. Nevertheless, the available devices cannot solve the issue of dependence on solar radiation. Finally, the results are limited to the

realization of the summer cycle without the solar radiation simulator in the compensated calorimetric chamber, and we could not evaluate the effect on visual comfort.

5. Conclusions

The experiment has been performed on a four-pane window system to investigate the dynamic thermal performance in the summer conditions. The surface temperature and the heat flux were measured on the interior and exterior sides of the sample. In summer conditions with a high outdoor air temperature of 35 °C, the temperature on the interior surface of the PCM window panel fluctuated in the range of about 21–23 °C, which means the overheating risk is avoided and the heat transferred into the room through the PCM window panel is markedly reduced compared with the double glazing system, as described in the simulation model. The air temperature was −15 °C on the exterior side of the window when the solidification process was tested. This measurement confirmed the incongruent melting of the PCM.

The effect of the solar radiation will be the subject of future studies. The results of the simulation model introduced in this study created a flexible model that can be used to inspect the effect of many variables in the building envelope. The PCM window panel reduces heat transfer through the window than the double-glazing panel. The application of the PCM window panel can considerably reduce the need for cooling and reduce overheating in buildings. Nevertheless, it is necessary to report an inappropriate location of the PCM inside the whole space of the window cavity. A nucleation agent or method should be used to place the PCM in order to prevent the formation of sediment in the window.

Acknowledgments: This work was supported by the Ministry of Education, Youth and Sports of the Czech Republic within the National Sustainability Programme project No. LO1303(MSMT-7778/2014), by the European Regional Development Fund under the project CEBIA-Tech No. CZ.1.02/2.1.00/03.0089, and by the Internal Grant Agency of Tomas Bata University in Zlín under the project No. IGA/CebiaTech/2017/002.

Author Contributions: All authors worked together on the manuscript. Martin Koláček researched the literature, worked on the experiment, measured and collected the data, and wrote the manuscript. Hana Charvatova helped with the numerical experiment in COMSOL Multiphysics. All authors have approved the final manuscript.

Conflicts of Interest: The authors declare no conflict of interest.

References

1. Barzin, R.; Chen, J.J.J.; Young, B.R.; Farid, M.M. Application of PCM Underfloor Heating in Combination with PCM Wallboards for Space Heating using Price Based Control System. *Appl. Energy* **2015**, *148*, 39–48. [CrossRef]
2. Weinläder, H.; Klinker, F.; Yasin, M. PCM Cooling Ceilings in the Energy Efficiency Center—Passive Cooling Potential of Two Different System Designs. *Energy Build.* **2016**, *119*, 93–100. [CrossRef]
3. Evola, G.; Marletta, L.; Sicurella, F. A Methodology for Investigating the Effectiveness of PCM Wallboards for Summer Thermal Comfort in Buildings. *Build. Environ.* **2013**, *59*, 517–527. [CrossRef]
4. Tokuç, A.; Başaran, T.; Yesügey, S.C. An Experimental and Numerical Investigation on the use of Phase Change Materials in Building Elements: The Case of a Flat Roof in Istanbul. *Energy Build.* **2015**, *102*, 91–104. [CrossRef]
5. Goia, F. Thermo-Physical Behaviour and Energy Performance Assessment of PCM Glazing System Configurations: A Numerical Analysis. *Front. Archit. Res.* **2012**, *1*, 341–347. [CrossRef]
6. Grynning, S.; Goia, F.; Rognvik, E.; Time, B. Possibilities for Characterization of a PCM Window System using Large Scale Measurements. *Int. J. Sustain. Built Environ.* **2013**, *2*, 56–64. [CrossRef]
7. Li, S.; Sun, G.; Zou, K.; Zhang, X. Experimental Research on the Dynamic Thermal Performance of a Novel Triple-Pane Building Window Filled with PCM. *Sustain. Cities Soc.* **2016**, *27*, 15–22. [CrossRef]
8. Zalba, B.; Marín, J.M.; Cabeza, L.F.; Mehling, H. Review on Thermal Energy Storage with Phase Change: Materials, Heat Transfer Analysis and Applications. *Appl. Therm. Eng.* **2003**, *23*, 251–283. [CrossRef]
9. Baetens, R.; Jelle, B.P.; Gustavsen, A. Phase Change Materials for Building Applications: A State-of-the-Art Review. *Energy Build.* **2010**, *42*, 1361–1368. [CrossRef]

10. De Gracia, A.; Cabeza, L.F. Phase Change Materials and Thermal Energy Storage for Buildings. *Energy Build.* **2015**, *103*, 414–419. [CrossRef]
11. Mehling, H.; Cabeza, L.F. *Heat and Cold Storage with PCM: An Up to Date Introduction into Basics and Applications*; Springer: Berlin/Heidelberg, Germany, 2008.
12. Dincer, I.; Marc, R.A. *Thermal Energy Storage Systems and Applications*, 2nd ed.; John Wiley and Sons, Ltd.: Chichester, UK, 2011, ISBN 978-0-470-74706-3.
13. Tyagi, V.V.; Buddhi, D. Thermal Cycle Testing of Calcium Chloride Hexahydrate as a Possible PCM for Latent Heat Storage. *Sol. Energy Mater. Sol. Cells* **2008**, *92*, 891–899. [CrossRef]
14. Furbo, S. *Heat Storage with an Incongruently Melting Salt Hydrate as Storage Medium Based on the Extra Water Principle*; Technical University of Denmark: Lyngby, Denmark, 1980.
15. Porisini, F.C. Salt Hydrates used for Latent Heat Storage: Corrosion of Metals and Reliability of Thermal Performance. *Sol. Energy* **1988**, *41*, 193–197. [CrossRef]
16. Asdrubali, F.; Baldinelli, G. Thermal Transmittance Measurements with the Hot Box Method: Calibration, Experimental Procedures, and Uncertainty Analyses of Three Different Approaches. *Energy Build.* **2011**, *43*, 1618–1626. [CrossRef]
17. Manz, H.; Egolf, P.; Suter, P.; Goetzberger, A. TIM–PCM External Wall System for Solar Space Heating and Daylighting. *Sol. Energy* **1997**, *61*, 369–379. [CrossRef]
18. European Standard EN ISO 12567–1. *Thermal Performance of Windows and Doors-Determination of Thermal Transmittance by Hot Box Method—Complete Windows and Doors*; International Organization for Standardization: Prague, Czech Republic, 2011. Available online: https://www.iso.org/standard/50327.html (accessed on 7 July 2017).
19. European Standard EN ISO 8990. *Thermal Insulation/Determination of Steady State Thermal Transmittance Properties—Calibrated and Guarded Hot Box*; International Organization for Standardization: Prague, Czech Republic, 1998. Available online: https://www.iso.org/standard/16519.html (accessed on 7 July 2017).
20. Gao, D.; Deng, T. Energy storage: Preparations and physicochemical properties of solid-liquid Phase change materials for thermal energy storage. *Mater. Processes Energy: Commun. Curr. Res. Tech. Dev.* **2013**, *1*, 32–44.
21. Gerlich, V.; Sulovská, K.; Zálešák, M. COMSOL Multiphysics Validation as Simulation Software for Heat Transfer Calculation in Buildings: Building Simulation Software Validation. *Measurement* **2013**, *46*, 2003–2012. [CrossRef]
22. Nikishkov, G. *Introduction to the Finite Element Method*; University of Aizu: Fukushima Prefecture, Japan, 2003.
23. Heim, D. Isothermal Storage of Solar Energy in Building Construction. *Renew. Energy* **2010**, *35*, 788–796. [CrossRef]
24. Carbonari, A.; de Grassi, M.; di Perna, C.; Principi, P. Numerical and Experimental Analyses of PCM Containing Sandwich Panels for Prefabricated Walls. *Energy Build.* **2006**, *38*, 472–483. [CrossRef]
25. Muhieddine, M.; Canot, E.; March, R. Various Approaches for Solving Problems in Heat Conduction with Phase Change. Available online: http://arphymat.univ-rennes1.fr/publis/2009%20FVM%20Muhieddine.pdf (accessed on 6 July 2017).
26. CSN 73 0548. *Calculation of Thermal Load of Air-Conditioned Spaces*, International Organization for Standardization: Prague, Czech Republic, 1985.